

reduction included corrections for background, Lorentz polarization, and absorption effects. The latter were based on  $\psi$  scans of reflections near  $\chi = 90^\circ$ , and the minimum relative transmission coefficient was 95.38%. Of 4419 unique data, 3142 had  $I > 3\sigma(I)$  and were used in the refinement.

The structure was solved by heavy atom methods and refined by full-matrix least squares based upon  $F$  with weights  $\omega = \sigma^2(F_o)$ , by using the Enraf-Nonius SDP programs. Non-hydrogen atoms were refined anisotropically. Hydrogen atoms were located in difference maps and were included as fixed contributions with isotropic  $B = 6.0 \text{ \AA}^2$ . A secondary extinction coefficient refined to a value of  $2.8(4) \times 10^{-7}$ . Convergence was achieved with maximum shift/esd = 0.10,  $R = 0.033$ ,  $R_w$

= 0.056, error of fit = 1.684 for 263 variables, and the maximum residual density was  $0.37 \text{ e \AA}^{-3}$ . Coordinates are listed in Table II.

**Acknowledgment.** We warmly thank the National Institutes of Health for support of this work.

**Supplementary Material Available:** Complete tables of bond distances and bond angles, coordinates for hydrogen atoms, and anisotropic thermal parameters (6 pages); listing of structure factor amplitudes (19 pages). Ordering information is given on any current masthead page.

## $\pi$ -Electron Properties of Large Condensed Polyaromatic Hydrocarbons

S. E. Stein\* and R. L. Brown

Contribution from the Chemical Kinetics Division, Center for Chemical Physics, National Bureau of Standards, Gaithersburg, Maryland 20899. Received September 25, 1986

**Abstract:** Hückel molecular orbital (HMO) theory has been used to calculate energy level densities, bond orders, electron distributions, free valence, resonance energies, and heats of formation for several homologous series of large, hexagonally symmetric benzenoid polyaromatic molecules with well-defined edge structures containing up to 2300 carbon atoms. When extrapolated to the infinite limit, values for all properties converge to reasonable values. This is in contrast to several other  $\pi$ -electron theories that do not yield correct graphite limits. Carbon atoms at the edge of such large molecules are predicted to behave like those in small polynuclear aromatic molecules, with properties strongly dependent on local structure. Regardless of edge structure, interior carbons several bond lengths from an edge have properties similar to those in an infinite graphite sheet. Edge structure has a larger influence on heats of formation than that predicted by group additivity methods. Only a weak correlation was found between the energy of the highest occupied molecular orbital and the reactivity of the most reactive position.

### 1. Introduction

Graphite and many carbonaceous substances consist primarily of large polyaromatic molecules of varying size, shape, and edge composition. An understanding of the chemistry of graphite is hampered by the inability to isolate these large molecules for individual study. As a result, the chemistry of graphite is often treated phenomenologically. Reactivity is thought to involve edges, defects, and other "active" sites, although the chemical nature of these is a matter of speculation.

The molecules in graphite belong to a class of compounds whose electronic properties are characterized primarily by their networks of mobile  $\pi$ -electrons. The chemical behavior of molecules of this type has been studied both experimentally and theoretically for many years and is thoroughly understood. A number of semiempirical theories have been developed and successfully applied to a large number of relatively small  $\pi$ -electron molecules<sup>1-5</sup>, and to graphite itself considered as an infinite  $\pi$ -electron array.<sup>6</sup> Presumably, these theories should also apply to the large chemical structures present in graphitic substances.<sup>7</sup> If so, they could be used to develop structure-reactivity relations that in turn would

aid in devising reaction mechanisms for these materials. In view of this, we have been using several of these theories to predict properties of some very large polyaromatic compounds.<sup>8-10</sup> Our initial goals have been to compare theories and to examine their convergence behavior. This latter consideration is important since any reliable theory should extrapolate to the correct graphite limits. Early in our work we noticed that the edge structure and overall size of such compounds were critically important factors in determining their reactivity. Our efforts have since focused on separating and studying these two variables individually.

We have been examining two types of theories. The simplest are based on Kekulé structure counts. One of these, structure-resonance theory (SRT)<sup>5</sup> was applied to molecules containing as many as 16000 carbon atoms. Most properties predicted by SRT are consistent and reasonable. Local properties such as bond orders and aromaticity indices converge properly to graphite limits and appear to be qualitatively correct. Unfortunately, some overall molecular properties such as ionization potentials diverge with increasing size, and others such as resonance energies per electron converge to different values depending on edge structure. Another method that is mathematically related to SRT is perturbation molecular orbital (PMO) theory.<sup>2,3</sup> It predicts electron localization energies. These have been used as reactivity indices for substitution reactions. This method, however, makes the implausible prediction that localization energies are zero for all positions in a sufficiently large graphite-like layer.<sup>10</sup>

Molecular orbital techniques were the second of the theoretical types we tested. These are more versatile in that they yield orbital energies and wave functions for  $\pi$ -electrons from which a variety of electronic properties can be calculated. The oldest and simplest

(1) Salem, L. *The Molecular Orbital Theory of Conjugated Systems*; W. A. Benjamin: New York, 1966.

(2) Dewar, M. J. S. *The Molecular Orbital Theory of Organic Chemistry*, McGraw-Hill: New York, 1969.

(3) Dewar, M. J. S.; Dougherty, R. C. *The PMO Theory of Organic Chemistry*; Plenum: New York, 1975.

(4) Heilbronner, E.; Bock, H. *The HMO Model and Its Application*; Wiley-Interscience: New York, 1976.

(5) Herndon, W. C. *Israel J. Chem.* **1980**, *20*, 270.

(6) Kelly, B. T. *Physics of Graphite*; Applied Science Publishers: London, 1981.

(7) (a) Bradburn, M.; Coulson, C. A.; Rushbrooke, G. S. *Proc.—R. Soc. Edinburgh, Sect. A: Math. Phys. Sci.* **1948**, *62*, 336. (b) Coulson, C. A.; Rushbrooke, G. S. *Proc. R. Soc. Edinburgh, Sect. A: Math. Phys. Sci.* **1948**, *62*, 350. (c) Seitz, W. A.; Kelen, D. J.; Schmalz, T. G.; Garcia-Bach, M. A. *Chem. Phys. Lett.* **1985**, *115*(2), 139.

(8) Brown, R. L. *J. Comput. Chem.* **1983**, *4*, 556.

(9) Stein, S. E.; Brown, R. L. *Carbon* **23**, **1985**, 105.

(10) Stein, S. E.; Brown, R. L. *Molecular Structures and Energetics*; Liebman and Greenberg, Eds.; VCH Publishers, 1987; Chapter 2.

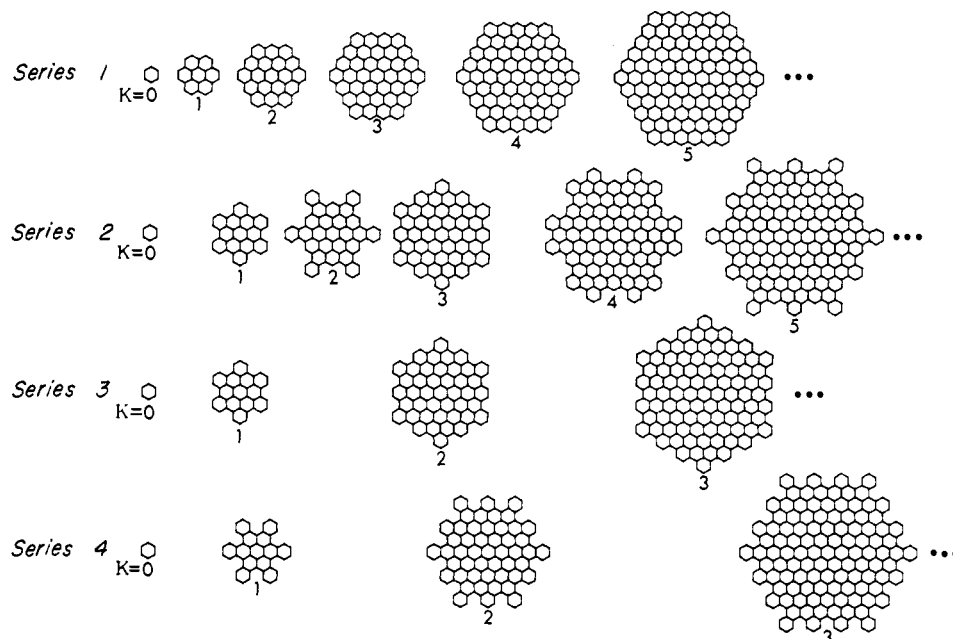


**Figure 1.** Homologous series of hexagonally symmetric molecules. In each series, a particular molecule can be identified by a generating index  $K$ . Benzene is the first member of each series and corresponds to  $K = 0$ . Various molecular properties can be expressed in terms of this index. For example, the number of carbon atoms  $N$  in series 1 molecules is given by the expression  $N = 6(K + 1)^2$ . Except in series 2, all molecules in a particular series have the same corner structure. Molecules in series 2 have three different corner structures: one for  $K = 0, 3, 6, \dots$ , a second for  $K = 1, 4, 7, \dots$ , and a third for  $K = 2, 5, 8, \dots$  note that the nature of the characteristic edge structure in series 2 is not clearly evident until one gets to molecules with  $K > 4$ .

of these is Hückel molecular orbital (HMO) theory.<sup>4</sup> Although its drastic assumptions and simplifications make it more a phenomenological model than a theory, its adjustable parameters allow it to fit a variety of experimental data. Benzenoid molecules in particular are accurately described by it. With minor reinterpretation<sup>11,12</sup> it has been used to establish a meaningful index of resonance stability, a task for which the original version was unsuccessful. We have used HMO theory to calculate energy level densities, bond orders, electron distributions, free valence (a reactivity index), resonance energies, and heats of formation<sup>13</sup> for several homologous series of large benzenoid polyaromatic molecules. Coulson and Taylor<sup>14</sup> have applied HMO theory to graphite considered as an infinite  $\pi$ -electron network. They calculated the  $\pi$ -electron energy per carbon atom, the density of states in the  $\pi$ -electron band, and the  $\pi$ -bond order. Their results are consistent with known properties of a single layer of graphite. Our calculated values for these properties in finite molecules all extrapolate to the Coulson and Taylor limits.

In addition, we also did similar calculations using a self-consistent field (SCF) version<sup>15</sup> of MO theory. Generally, this gave predictions similar to those of HMO theory. It is of course far more computationally intensive. Unfortunately, in the graphite limit, it yielded a nonzero band gap<sup>10</sup> and alternating carbon-carbon bond lengths. Both of these predictions contradict observation. We have not been able to modify our SCF calculations to correct these problems.

At present, of all the theoretical techniques that we have examined, we feel that the classical HMO method is the most reliable one for our purposes. It is computationally simple, gives reasonable accounts of the electronic properties of small benzenoid molecules, and converges to the correct infinite plane limits. There is no obvious reason why it should not be equally valid for benzenoid molecules of intermediate size. We report here results of our HMO calculations on several series of large benzenoid polyaromatic molecules.

## 2. Computational Approach

As in our earlier work, we examined four homologous series of hexagonally symmetric molecules. Each series consists of a sequence of increasingly larger molecules all of which have the same edge structure. Use of such homologous series facilitates the extrapolation of the various electronic properties to infinite size (graphite). The first few members of each series are shown in Figure 1. Edge carbon valences are assumed to be satisfied by hydrogen atoms. We find that the four different edge structures shown here represent most of the possible local configurations. The high degree of symmetry possessed by these molecules made it possible to use group theoretical methods. This greatly simplified the problem of applying HMO theory to very large molecules. Our computational methods are documented in detail elsewhere.<sup>17</sup> The largest molecules for which a complete calculation was performed, giving both energy levels and wave functions, contained 1014 carbon atoms, the largest for which only energies were determined contained 2314 carbons. Limits on the size of the molecules we could treat were determined by the memory of our computer and not by computation times. Note that all molecules considered here are even-alternant benzenoid hydrocarbons.

## 3. Results and Discussion

Our previous calculations,<sup>9,10</sup> which were based on Kekulé structure counts, indicated that the edge structure of these hydrocarbons was a key factor influencing their thermodynamic stability and chemical reactivity. Series 1 molecules with their anthracene-like edges were thermodynamically unstable and highly reactive. This edge type blocked  $\pi$ -electron conjugation. In these molecules, regions near the edge resembled polyolefins more than they did polyaromatics. In contrast, series 2 and 3 had edges consisting of the most stable structures possible. They were "fully benzenoid"<sup>18</sup> while series 1 molecules were not. Series 4 molecules

(11) Hess, B. A., Jr.; Schaad, L. J. *J. Am. Chem. Soc.* **1971**, *93*, 2413.

(12) Hess, B. A., Jr.; Schaad, L. J. *Pure Appl. Chem.* **1980**, *52*, 1471.

(13) Schaad, L. J.; Hess, B. A., Jr., *J. Am. Chem. Soc.* **1971**, *94*, 3068.

(14) Coulson, C. A.; Taylor, R. *Proc. Phys. Soc., London, Sect. A* **1952**, *65*, 815.

(15) Dewar, M. J. S.; de Llano, C. J. *J. Am. Chem. Soc.* **1969**, *91*, 789.

(16) This appears to be a characteristic of SCF methods. See: Kertész, M. *Adv. Quantum Chem.* **1982**, *15*, 161.

(17) Brown, R. L. *Application of Semi-Empirical SCF-MO Theory to Very Large Hexagonally Symmetric Benzenoid Polyaromatic Hydrocarbons*; U.S. National Bureau of Standards International Report, **1985**, NBSIR 85-3244. The HMO energies and wave functions are given by the zeroth order calculations in the SCF method described here.

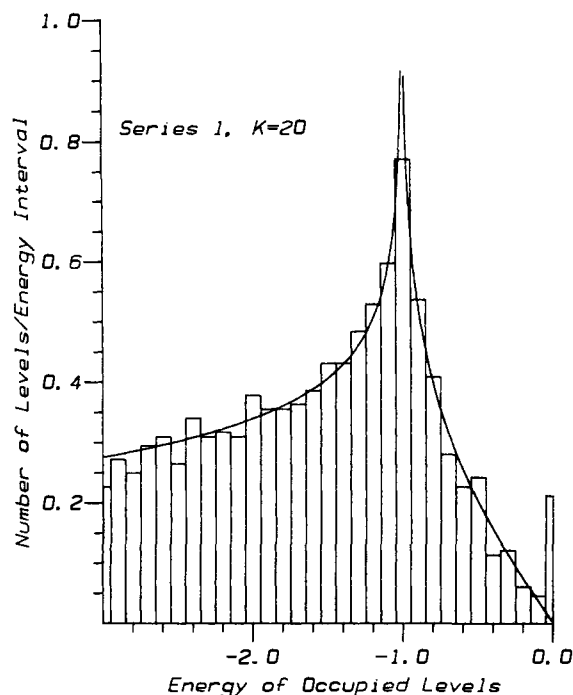


**Figure 2.** Histogram showing density of occupied HMO orbital energy levels as a function of energy for a molecule with 2646 carbons and anthracene edge type. The smooth curve shows the graphite limit. Since we use classical HMO theory, with zero differential overlap, the unoccupied levels need not be shown as they have the same density relative to the energy zero as the occupied levels. The energy zero is that of an electron in a  $2p_z$  orbital. Energy units are  $\beta$ , the Hückel resonance integral.

fell between these two extremes. As we shall see in what follows, most of these earlier conclusions are confirmed by the HMO calculations.

**3.1. Energy Levels.** Calculating only the orbital energies of these molecules is easier than determining both their energies and wave functions. Consequently, convergence limits for energies may be approached more closely since larger molecules can be treated. In the following section, we consider (1) the densities of occupied orbitals, (2) the energies of the highest occupied molecular orbital (HOMO), (3) resonance energies, and (4) heats of formation.

**3.1.1. Orbital Level Densities.** The total number of occupied energy levels in these molecules is equal to  $N/2$ , where  $N$  is the number of  $\pi$ -electrons. Each level is occupied by two electrons. As  $N$  goes to infinity, we expect the energy level distributions for the molecules in each of the different series to approach that for the infinite plane. The density of states for the infinite plane has been given in integral form by Coulson and Taylor.<sup>14</sup> We can compare our results for large finite molecules with this limiting case. In Figures 2 and 3, we show in the form of histograms, the numbers of occupied levels in any energy interval  $0.1\beta$  ( $\beta =$  Hückel resonance integral) as a function of orbital energy  $E$ . These are scaled so that the area under the histogram is unity. (At the ends of the energy range, interval sizes were set to  $0.05\beta$  so that  $E = 1\beta$  would fall at the center of a  $0.1\beta$  interval.) Similar sized molecules, one from the least and another from the most stable series, are shown.

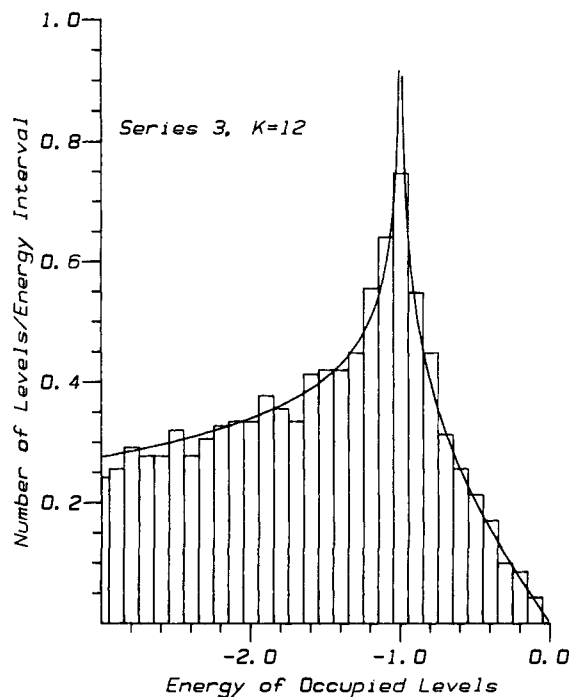


**Figure 3.** Histogram showing density of occupied HMO orbital energy levels as a function of energy for a molecule with 2814 carbons and a phenanthrene edge type.

The least stable case, given in Figure 2, is a series 1 molecule having index  $K = 20$  and 2646 carbon atoms. The smooth curve gives the limiting infinite plane distribution. Except in the highest energy interval, the densities are close to the limiting curve. As a representative of the most stable series 3, we consider  $K = 12$  with 2314 carbons. Its level density histogram is shown in Figure 3. Here the densities are all close to the infinite plane limit. Both histograms show some density fluctuations about the graphite limit. These are expected to diminish as one goes to larger molecules.

In series 1, all of its molecules that we examined (these had  $K = 12$  through 20) showed a large excess of levels near the energy zero. In the limit as  $K$  goes to infinity, of course, the abnormally high density here should vanish. That this would occur was not obvious from a cursory look at the histograms for these molecules. To better establish this assertion, we tabulated the number of occupied energy levels,  $N_{0.05}$ , in the top  $0.05\beta$  energy interval of these nine molecules. We found  $N_{0.05} = K - 6$  unless  $K$  is a multiple of 3, in which case  $N_{0.05} = K - 7$ . The density of levels in this interval,  $D_{0.05}$ , is proportional to the ratio of  $N_{0.05}$  to the total number of occupied levels which is  $3(K + 1)^2$  for this series. Therefore, if the above formula for  $N_{0.05}$  remains valid as  $K$  goes to infinity, we would then have  $D_{0.05}$  going to zero slowly as  $10K$ . The abnormally high density in this region will thus eventually disappear.<sup>19</sup>

Energy level densities for the other two homologous series were also calculated. Series 2 has a distribution like that of series 3 while series 4, like series 1, has an abnormally high concentration of levels near the energy zero.

**3.1.2. Energy of Highest Occupied Orbital.** Of particular interest is the energy of the highest occupied molecular orbital,  $E_{\text{HOMO}}$ , and that of the lowest empty orbital, the latter being equal to  $-E_{\text{HOMO}}$  for the even-alternant compounds considered here. These are related to the hydrocarbon's ionization and reduction potentials, respectively. Their positions can also be related to the compound's color and electrical conductivity and have been used as a general indicator of chemical reactivity. In graphite, as we see from the limiting curve shown in Figures 2 and 3,  $E_{\text{HOMO}}$  equals zero, there being no energy gap between the highest oc-

(18) Clar, E. J. *Polycyclic Hydrocarbons*; Academic: New York, 1964; Vol. 1, pp 26-27. A fully benzenoid molecule, as defined by Clar, is one that can be fully decomposed into independent benzenoid rings (or into *p*-polyphenyl chains). These molecules are always found to be relatively unreactive. The most stable depictions of benzenoid polycyclic molecules are those that are composed of the largest number of isolated benzenoid rings, subject to the constraint that each aromatic carbon atom not part of a benzenoid ring can be assigned to a distinct double bond. Only about one-half of the carbon atoms in large series 1 molecules could be assigned to benzenoid rings. In large series 2 molecules, about three-quarters of the carbon atoms could be assigned to benzenoid rings.

(19) The correct limiting value of  $D_{0.05}$  is not zero but 0.009. This requires that there be a small, and probably changing, term in the relation for  $N_{0.05}$  which is proportional to  $K^2$ . Over the limited range  $K = 12-20$  such a small term was not detectable.

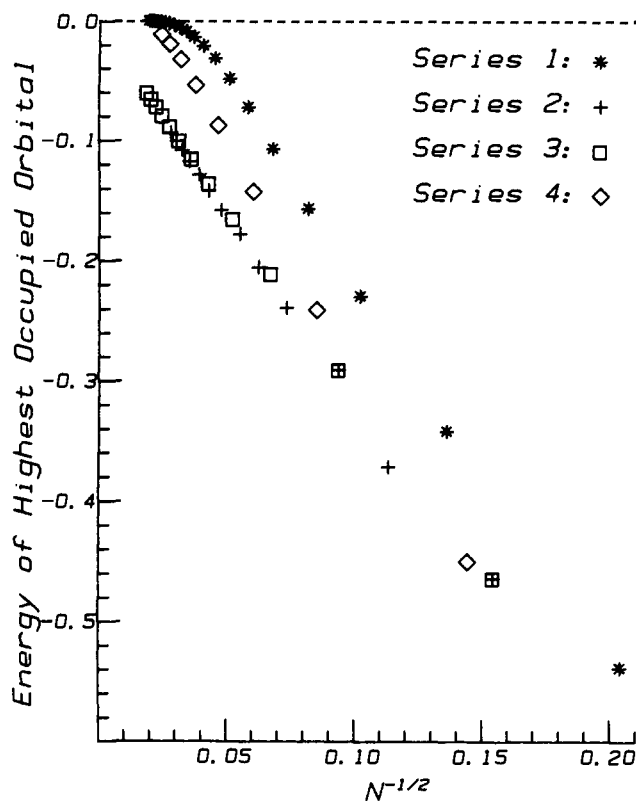


**Figure 4.** Energy of highest occupied molecular orbital (HOMO) as a function of molecular size. The reciprocal of the square root of the number  $N$  of  $\pi$ -electrons in the molecule was used for the abscissa. This was done to expand the scale near the origin (i.e., where  $N$  goes to infinity). Energy is in units of  $\beta$ .

occupied and lowest empty orbitals. For all of our homologous series, the values of  $E_{\text{HOMO}}$  extrapolate to zero as  $N$  goes to infinity. However, as shown in Figure 4, the rate of approach to this limit varies among the different series. Noteworthy are the two fully benzenoid series (2 and 3) where  $E_{\text{HOMO}}$  values approach zero very slowly. For molecules with these edges, reaction rates sensitive to the ease of oxidation or reduction would not reach limiting values until the molecules reached a very large size. The general unreactive nature of fully benzenoid molecules is of course consistent with experimental observations on reactivities of smaller polyaromatic hydrocarbons.<sup>20</sup>

**3.1.3. Resonance Energy.** Resonance energy in a  $\pi$ -electron system can be defined as the difference between its total  $\pi$ -electron energy and the energy it would have if its  $\pi$ -electrons were in some sense localized in definite bonds. This localized reference structure has been defined in various ways. The approach we adopt here is that proposed by Hess and Schaad.<sup>11</sup> They classified both double and single carbon-carbon bonds into eight types depending on their numbers of attached hydrogens. For acyclic polyenes, they found that the  $\pi$ -electron energy calculated by HMO theory is a linear function of these bond types. Consequently, they were able to assign a  $\pi$ -bond energy,  $E_{ij}$ , to each of these types. For a cyclic hydrocarbon the HMO  $\pi$ -energy is usually not additive in the bonds. They define its resonance energy as the difference between its HMO energy and its additive energy obtained by summing the individual bond energies  $E_{ij}$ . They find that this definition of resonance energy gives excellent correlations with the chemical behavior and stability of a variety of  $\pi$ -electron compounds.

Resonance energies per  $\pi$ -electron (REPE) for the molecules in our four series are shown in Figure 5 as a function of molecular size. Details of the reference energy calculations are given in the Appendix. In graphite, the average  $\pi$ -energy per carbon has been given in the form of a double integral by Coulson and Taylor.<sup>14</sup>

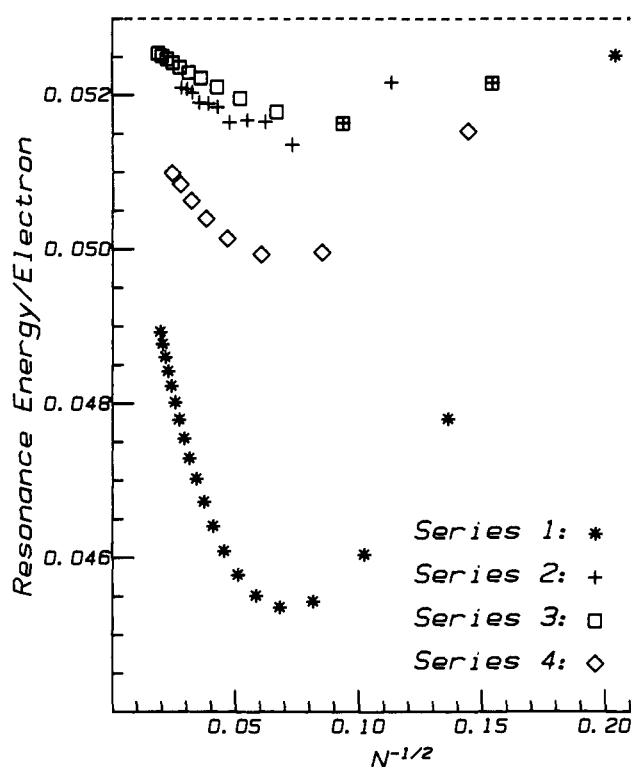


**Figure 5.** Resonance energy per  $\pi$ -electron as a function of molecular size. The dotted line shows the graphite limit.

The result is  $1.57460\beta$ .<sup>21a</sup> For the localized reference graphite structure, the additive  $\pi$ -energy per carbon is  $1/2E_{20} + E_{10} = 1.5216\beta$ , where  $E_{20}$  and  $E_{10}$  are the Hess and Schaad bond energies for C=C and C-C, respectively. The REPE for graphite is thus  $0.0543\beta$ , in exact agreement with the value obtained by Hess and Schaad.<sup>21b</sup> In all our series, the REPE values initially decrease as we go to larger molecules. They all experience minima, however, in the vicinity of  $N = 240$ . For large  $N$ , they increase and all eventually reach the graphite limit. Relative resonance stabilities are the same as those predicted by the simpler theories<sup>9,10</sup> with series  $1 < 4 < 2 \approx 3$ .

For a series of small benzenoid hydrocarbons, Hess and Schaad<sup>11</sup> found a linear correlation between REPE and the energy of the highest occupied molecular orbital. An examination of Figures 4 and 5 shows that this correlation is not valid for larger molecules.

**3.1.4. Heats of Formation.** Schaad and Hess<sup>13</sup> have used HMO  $\pi$ -energies  $E_{\text{HMO}}$  to calculate heats of atomization. They fit a three-parameter expression which contains  $E_{\text{HMO}}$  to the observed heats of atomization of ten polybenzenoid compounds. Although adequate for small molecules, this parameterization does not converge properly to the infinite plane limit. To correct this problem, we have developed a slightly different parameterization scheme. In what follows, we use heats of formation rather than heats of atomization.

The standard gas phase heat of formation of our molecules is given by

$$\Delta H_f(g, C_N H_M) = N\Delta H_f(g, C) + M\Delta H_f(g, H) - \Delta H_a(g, C_N H_M) \quad (1)$$

Schaad and Hess<sup>13</sup> have assumed that the heat of atomization  $\Delta H_a(g, C_N H_M)$  can be approximated by the three-power expression

$$-\Delta H_a(g, C_N H_M) = -ME_{\text{CH}} - N_{\text{CC}}E_{\text{CC}} - \gamma E_{\text{HMO}} \quad (2)$$

(21) (a) This value is slightly different from that calculated by Coulson and Taylor.<sup>14</sup> It results from a reevaluation of their integral for the average energy whose integrand contains an elliptic integral. We used a polynomial approximation for this elliptic integral. (See: Abramowitz, M.; Stegun, I. A. *Handbook of Mathematical Functions*; U.S. National Bureau of Standards Applied Mathematics Series 55, 1964; p 592.) (b) Hess, B. A.; Schaad, L. J. *J. Org. Chem.* **1986**, *51*, 3902.

**Table I.** Comparison of Calculated and Experimental  $\Delta H_f$  (298 K)

compd	steric terms		$\Delta H_f(\text{exptl})^a$	$\Delta H_f(\text{exptl}) - \Delta H_f(\text{calcd})$	exptl precisn
	$S_1$	$S_2$			
benzene	0		19.8	-0.1	0.13
naphthalene			35.8	0.5	0.25
anthracene			54.4	1.5	1.1
phenanthrene	1		50.0	0.7	1.1
naphthacene			67.8	-3.4	1.1
benz[a]anthracene	1		66.0	0.0	1.0
chrysene	2		62.8	-1.4	1.2
triphenylene	3		61.9	-1.0	1.1
pyrene			53.7	-0.3	0.4
perylene	2		73.7	2.3	1.1
benzo[c]phenanthrene		1	69.6	0.0	1.2
average				1.0	0.9

<sup>a</sup> Experimental values are from ref 27 except for that of pyrene which comes from ref 22.

where  $E_{\text{CH}}$  is an average bond energy for the CH bonds and  $E_{\text{CC}}$  is an average  $\sigma$ -bond energy for the C-C bonds. The  $\pi$ -bonding energy is  $E_{\text{HMO}}$ . They have shown the  $\sigma$ -compression energies for the C-C bond need not be explicitly considered since they are proportional to  $E_{\text{HMO}}$  and can thus be incorporated into the parameter  $\gamma$ .

In the graphite limit, we have for the heat of formation per carbon atom

$$\begin{aligned} (\Delta H_f/N)_{N \rightarrow \infty} &= \Delta H_f(\text{g,C}) - E_{\text{CC}}(N_{\text{CC}}/N)_{N \rightarrow \infty} - \\ &\quad \gamma(E_{\text{HMO}}/N)_{N \rightarrow \infty} \\ &= \Delta H_f(\text{g,C}) - 1.5E_{\text{CC}} - 3P_g\gamma \end{aligned} \quad (3)$$

where  $P_g$  is the bond order in graphite; it equals<sup>14,21</sup> 0.524 866. Since the heat of formation of graphite is defined as zero, this limit is equivalent to the heat of sublimation per carbon of an infinitely large benzenoid polyaromatic hydrocarbon. This could be viewed as a "gaseous" single graphite layer. If the  $E_{\text{CC}}$  and  $\gamma$  parameter values obtained from a fit of the first ten compounds in Table I are used in,<sup>3</sup> one gets  $(\Delta H_f/N)_{N \rightarrow \infty} = 2.6$  kcal/mol. This is considerably higher than the 1.45 kcal/mol which has been observed for the heats of sublimation of large polyaromatics.<sup>22-24</sup>

To assure proper convergence, we use<sup>3</sup> with the observed value of  $(\Delta H_f/N)_{N \rightarrow \infty}$  to eliminate one of its parameters. In addition, to improve the fit of the data in Table I, we find it necessary (and logical) to introduce two steric terms in the manner of Herndon.<sup>26</sup> These are shown in Table I for the fitted compounds. Variable  $S_1$  refers to the close H,H interaction of the type observed in phenanthrene;  $S_2$  refers to one of the type found in benzo[c]phenanthrene. Our resulting formula is

$$\Delta H_f = [q_1N + q_2M - 2(q_1 - q_3)N_{\text{CC}}/3] - Mp_1 + (2P_gN_{\text{CC}} - E_{\text{HMO}})p_2 + S_1p_3 + S_2p_4 \quad (4)$$

where  $q_1 = \Delta H_f(\text{g,C})(298 \text{ K}) = 170.866$  kcal/mol,<sup>27</sup>  $q_2 = \Delta H_f(\text{g,H})(298 \text{ K}) = 52.10$  kcal/mol,<sup>27</sup> and  $q_3 = 1.45$  kcal/mol. Parameters  $p_1$ ,  $p_2$ , and  $p_3$  were obtained by least-squares fit of the first ten compounds in Table I; reciprocals of the experimental uncertainties shown there were used as weighting factors. Parameter  $p_4$  was then determined by correcting the predicted  $H_f$  for benzo[c]phenanthrene to its experimental value. The values (kcal/mol) obtained were  $p_1 = 94.2592$ ,  $p_2 = 43.9060$ ,  $p_3 = 2.2606$ , and  $p_4 = 9.67$ . The average deviation of the fitted values was 1 kcal/mol which compares favorably with those obtained with other estimation schemes.<sup>28</sup>

(22) Smith, N. K.; Stewart, R. C.; Jr., Osborn, A. G.; Scott, D. W. *J. Chem. Thermodyn.* **1980**, *12*, 919.

(23) Malaspina, L.; Bardi, G.; Gigli, R. *J. Chem. Thermodyn.* **1974**, *6*, 1053.

(24) Stull, D. R.; Westrum, E. F., Jr.; Sinke, G. C. *The Chemical Thermodynamics of Organic Compounds*; Wiley: New York, 1969.

(25) DeKruif, C. G. *J. Chem. Thermodyn.* **1980**, *12*, 243.

(26) Herndon, W. C. *Thermochim. Acta* **1974**, *8*, 225.

(27) Cox, J. D.; Pilcher, G. *Thermochemistry of Organic and Organometallic Compounds*; Academic: New York, 1970.

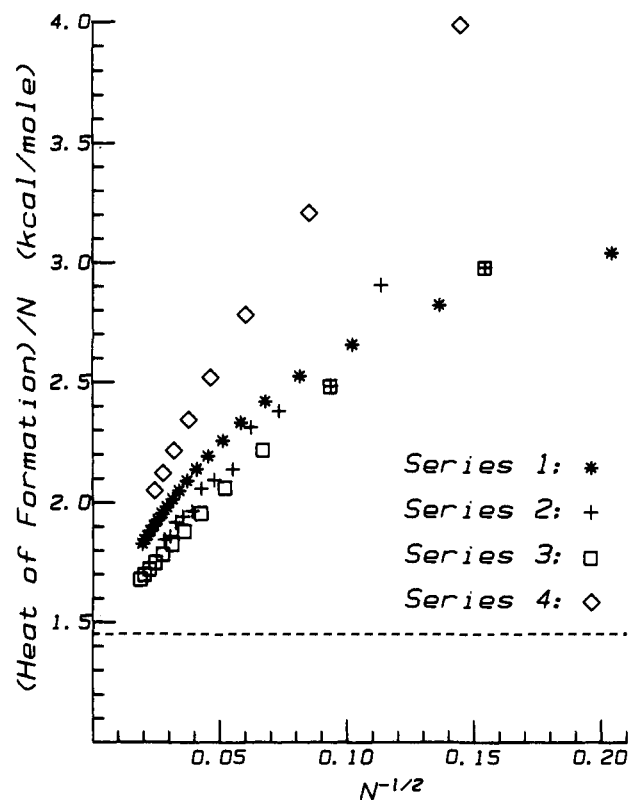


**Figure 6.** Heat of formation per carbon as a function of molecular size. The dotted line shows the graphite limit.

Heats of formation per carbon for our four homologous series of compounds are shown in Figure 6 as a function of molecular size. This method predicts appreciable differences between the thermodynamic stabilities of the different series. This is in contrast to the group additivity approach<sup>28</sup> which predicts very little difference in the stabilities of molecules of comparable size.<sup>10</sup> For example, the present method gives for the series 1 compound with 1014 carbons a heat of formation 188 kcal/mol higher than that for the series 3 compound with the same number of carbons. In contrast, the group additivity method gives 30 kcal/mol for this difference. By design, both methods give the same results in the graphite limit.

**3.2. Wave Functions.** A complete solution of the HMO problem gives the orbital wave functions from which a number of electronic properties may be calculated. We consider here (1)  $\pi$ -bond orders and their convergence limits, (2)  $\pi$ -electron distributions, in particular, those of the highest occupied molecular orbital (HOMO), the so-called frontier orbitals, and finally (3) the free valence at each carbon center. This is a reactivity index which is useful for correlating with the position and ease of radical and electrophilic attack.

**3.2.1. Bond Orders.** The  $\pi$ -bond orders for two molecules are shown in Figures 7 and 8. These are plotted as a function of the distance of a particular bond's midpoint from the center of the molecule. Both molecules have 1014 carbons. The first is from series 1 and the second from series 3. The dotted line gives the graphite bond order. In both molecules the bond orders are close to the graphite limit for all but the bonds near the edges. At the edges, the pattern of shorter and longer bonds is the same as that predicted by the simple structure resonance theory (SRT).<sup>10</sup> However, the magnitudes of the predicted variations are much less. In particular, for series 1 molecules, with their anthracene-type edge, SRT predicted a very strong bond alternation along the edge. This was greatest at the corners and diminished only slowly toward the edge center. In contrast, HMO bond orders in this molecule are uniform along most of the edge. Only near

(28) Stein, S. E.; Golden, D. M.; Benson, S. W. *J. Phys. Chem.* **1977**, *81*, 314.

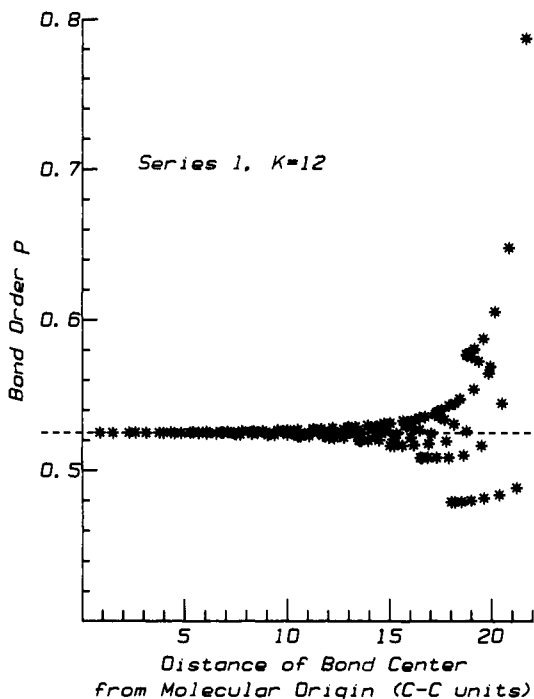


Figure 7. Bond orders across a series 1 molecule (anthracene edge type),  $N = 1014$ . Distance unit is graphite C-C length.

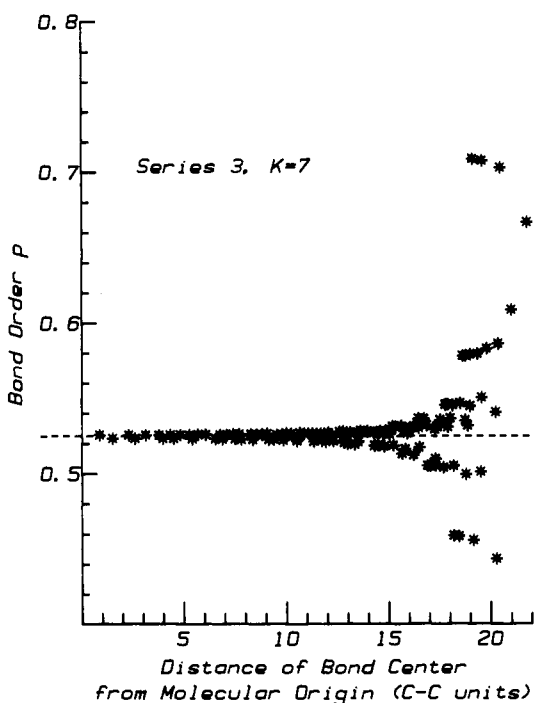


Figure 8. Bond orders across a series 3 molecule (phenanthrene edge type),  $N = 1014$ . Distance unit is graphite C-C length.

the corners does bond alternation become appreciable.

Convergence behavior of the bond orders of the center six symmetrically equivalent bonds in each molecule is shown in Figure 9. Note the expanded scale; its whole range equals one division in Figures 7 and 8. For all molecules, these bond orders are very close to the graphite limit although they approach it at different rates. Even rather small molecules such as coronene (not shown on this plot) have center bond orders which are close to that of graphite.

**3.2.2. Electron Distributions.** Because of the large number of occupied orbitals in these big molecules, it was not feasible to examine the  $\pi$ -electron distribution in each orbital. Instead, we calculated the average position of an electron in a particular orbital. From this, those orbitals having unusual electron dis-

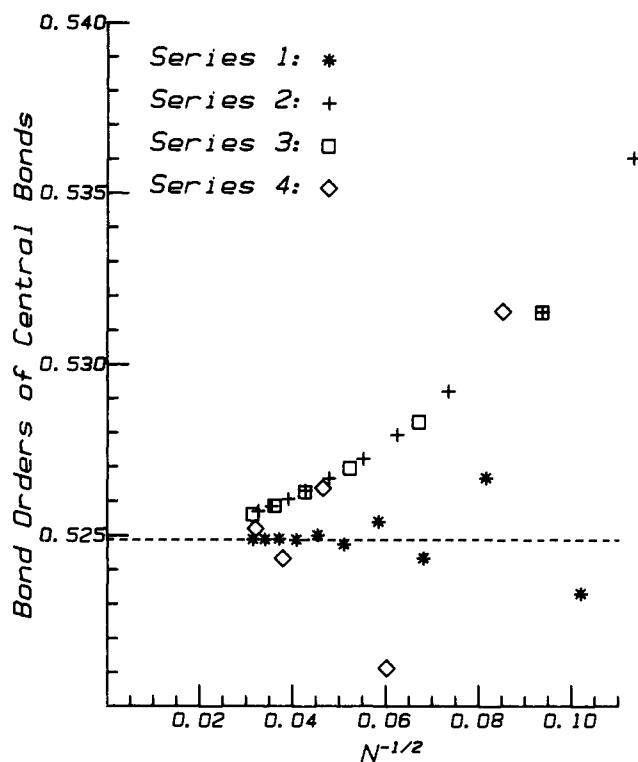


Figure 9. Bond orders of center six symmetrically equivalent bonds vs. molecular size. Dotted line gives graphite limit.

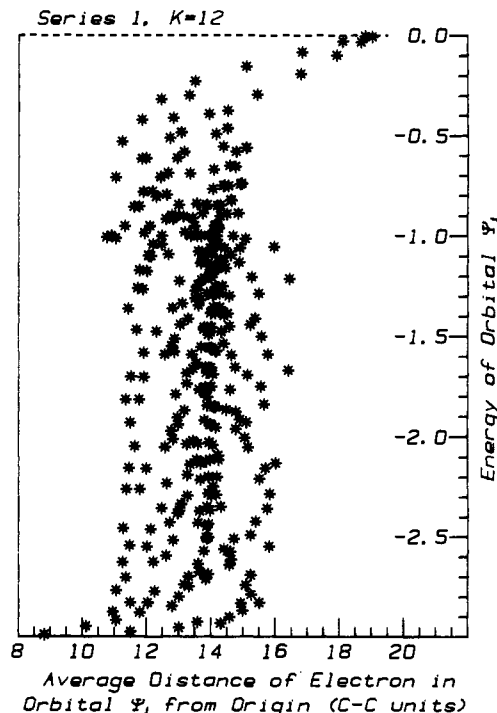
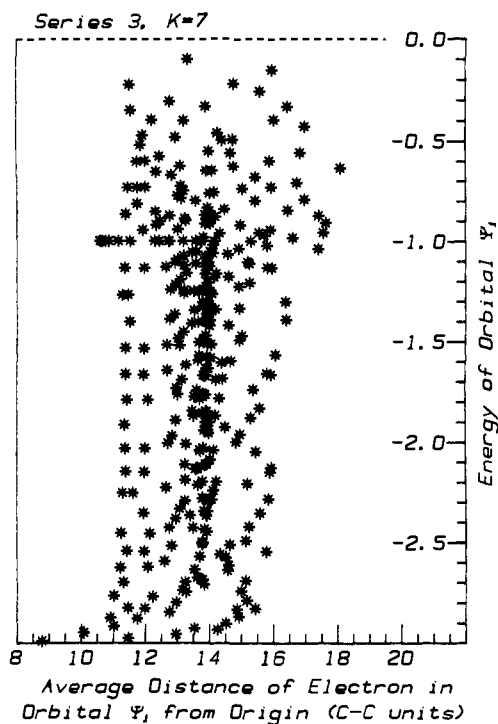


Figure 10. Orbital energies as a function of the average distance of an electron from the molecular center. Molecule is from series 1 with  $K = 12$  and  $N = 1014$ . If the electron's distribution in an orbital were completely uniform, its average distance from the origin would be 13.684 graphite C-C lengths.

tributions could easily be identified. The energy of a particular orbital is shown in Figures 10 and 11 as a function of the average distance of an electron in this orbital from the molecule's center. The molecules are the same as those discussed in the last section.

These diagrams exhibit very clearly the marked effects of edges on the  $\pi$ -electron distributions. Although both molecules have the same shape and size, only for orbitals below energies of  $-2$  are the electron distributions similar. At the highest levels in



**Figure 11.** Orbital energies as a function of the average distance of an electron from the molecular center. Molecule is from series 3 with  $K = 7$  and  $N = 1014$  carbons. If the electron's distribution in a particular orbital were completely uniform, its average distance from the origin would be 13.690 graphite C-C lengths.

particular, the differences are striking. For molecules having anthracene-like edges (series 1) the  $\pi$ -electron in the highest orbital is concentrated at the perimeter. Furthermore, this concentration of electron probability at the edges is not limited to the highest level. It is evident in all of the highest six or seven orbitals. In contrast, electrons in high orbitals of molecules with phenanthrene-like edges are uniformly distributed over the whole structure.

The complete wave functions for the HOMOs of two smaller molecules, one from series 1 and the other from Series 3, are shown in Figures 12 and 13. In parts a-c of Figure 12, we have the series 1 molecule with  $K = 5$  and  $N = 216$ . This HOMO is doubly degenerate. The first two diagrams, a and b, show the magnitudes and signs of the atomic orbital coefficients,  $C_i(a)$  and  $C_i(b)$ , at carbon center  $i$ , for the pair of wave functions associated with the orbital. The third diagram c is an average of the first two; its coefficients,  $C_i$ , are simply  $C_i^2 = (C_i(a)^2 + C_i(b)^2)/2$ . Even in this smaller molecule the concentration of HOMO electron density at the edges is quite pronounced.

In parts a-c of Figure 13, we show the same types of diagrams for the HOMO of a series 3 molecule with  $K = 3$  and  $N = 222$ . Here the average distribution is quite uniform over the whole molecule.

For larger members of series 1, this shift in HOMO electron distribution toward the edge is greater. HOMO distributions are shown in Figures 14 and 15 for the  $N = 1014$  molecules previously illustrated in Figures 7, 8, 10, and 11. For these large molecules, complete wave function diagrams are not feasible. Because of the hexagonal symmetry, each carbon center in these molecules falls into a particular set of symmetrically equivalent carbons. Each center in the set is at the same distance from the molecule's origin and all have the same orbital coefficients. At center  $i$ , the average relative electron probability is  $N(C_i(a)^2 + C_i(b)^2)/2$ . This quantity was plotted as a function of distance from the origin for each equivalent set of carbons. For series 1,  $K = 12$ , the result is shown in Figure 14. The inset shows the distribution on a reduced scale so that the full magnitude of the probabilities can be seen. Essentially all of the distribution lies at the edge. The main plot in Figure 14 is on the same scale as that used in Figure 15. Here we give the HOMO distribution for the series 3,  $K =$

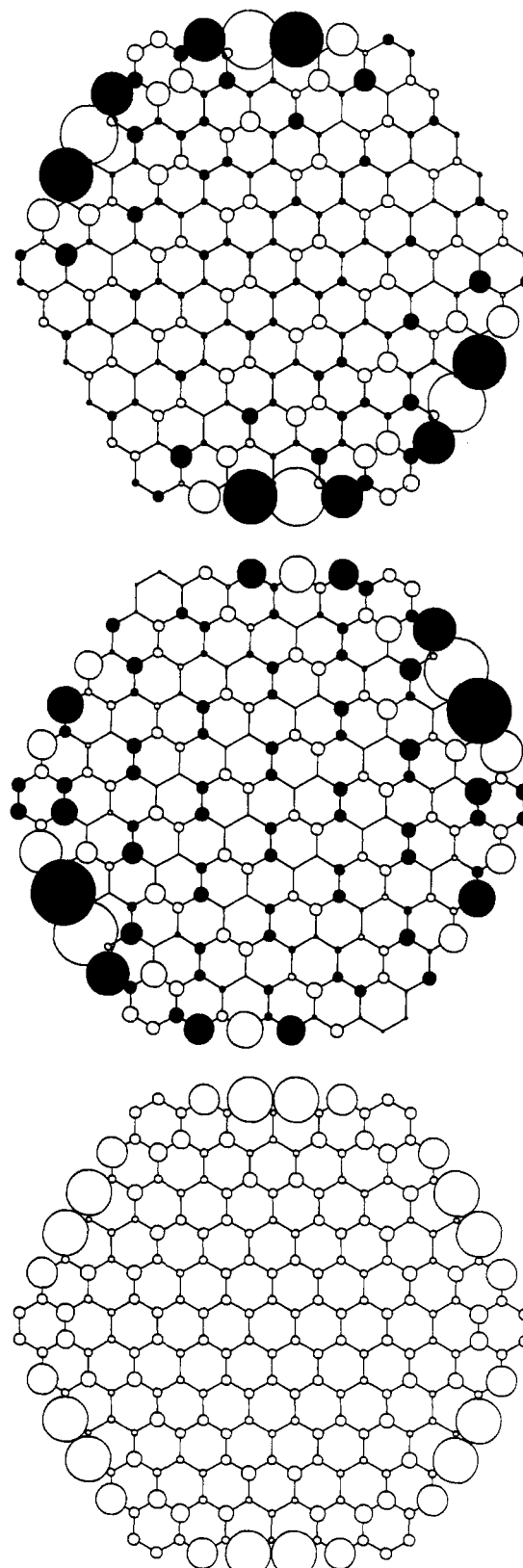


**Figure 12.** HOMO for series 1,  $K = 5$ ,  $N = 216$ , molecule. This orbital is doubly degenerate. (a and b) Pair of functions associated with degenerate orbital. (c) Average electron probability in this orbital.

7 molecule. As in the smaller member of this series shown in Figure 13c, the electron in this orbital is quite evenly distributed over the whole molecule.

**3.2.3. Free Valence.** Free valence<sup>4,29</sup> is a reactivity index that measures potential reactivity in a  $\pi$ -electron network. Carbon

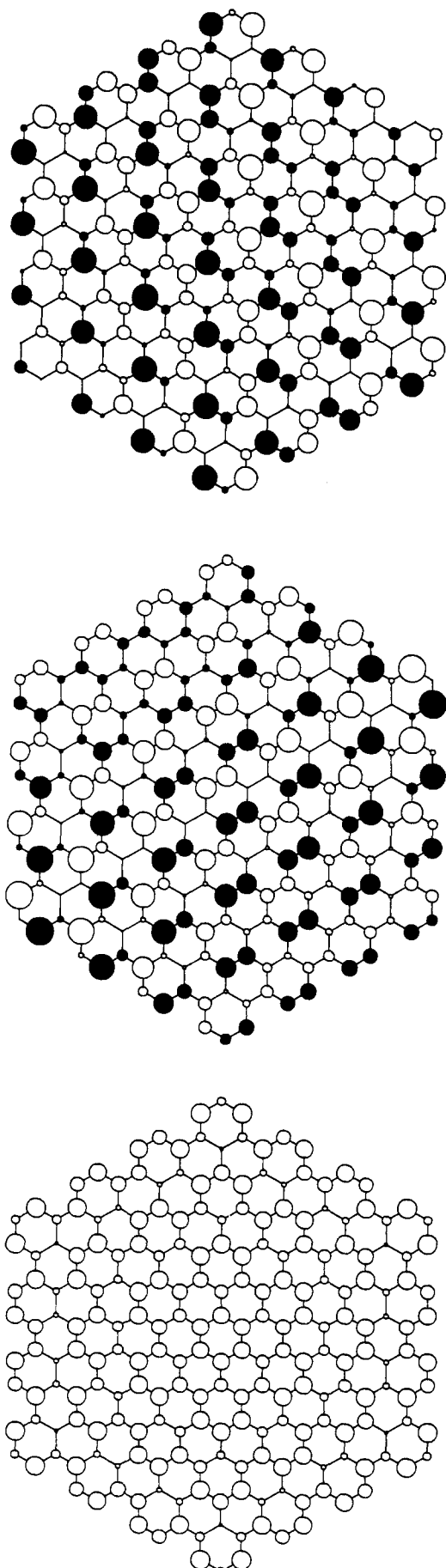


**Figure 13.** HOMO for series 3,  $K = 3$ ,  $N = 222$ , molecule. This orbital is doubly degenerate. (a and b) Pair of functions associated with degenerate orbital. (c) Average electron probability in this orbital.

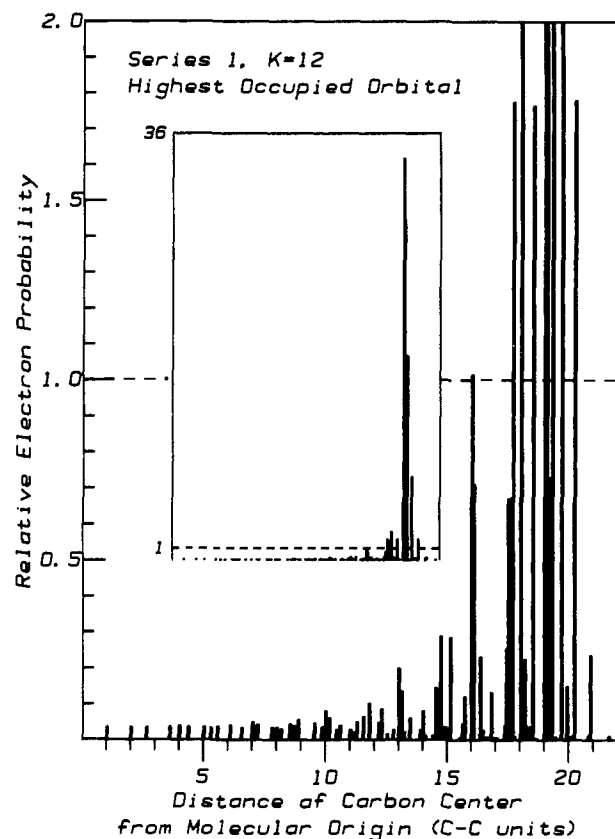


**Figure 14.** Average relative electron probability in HOMO of series 1,  $K = 12$ ,  $N = 1014$  molecule. Inset shows full distribution. Distance unit is graphite C-C length.

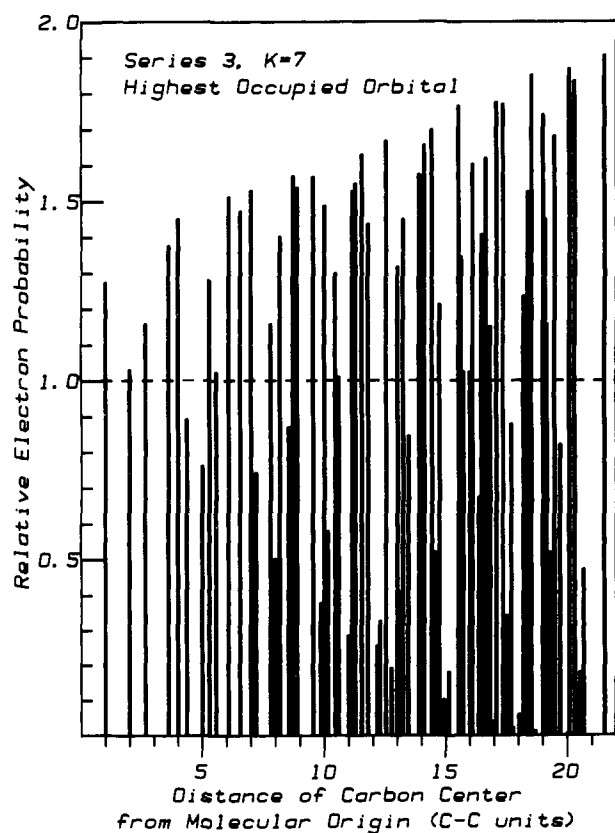


**Figure 15.** Average relative electron probability in HOMO of Series 3,  $K = 7$ ,  $N = 1014$  molecule. Distance unit is graphite C-C length.

atoms in positions of high reactivity are assumed to be those which have weak  $\pi$ -bonds with their neighbors. For a given center  $i$ , free valence is defined as the maximum theoretical total bond order



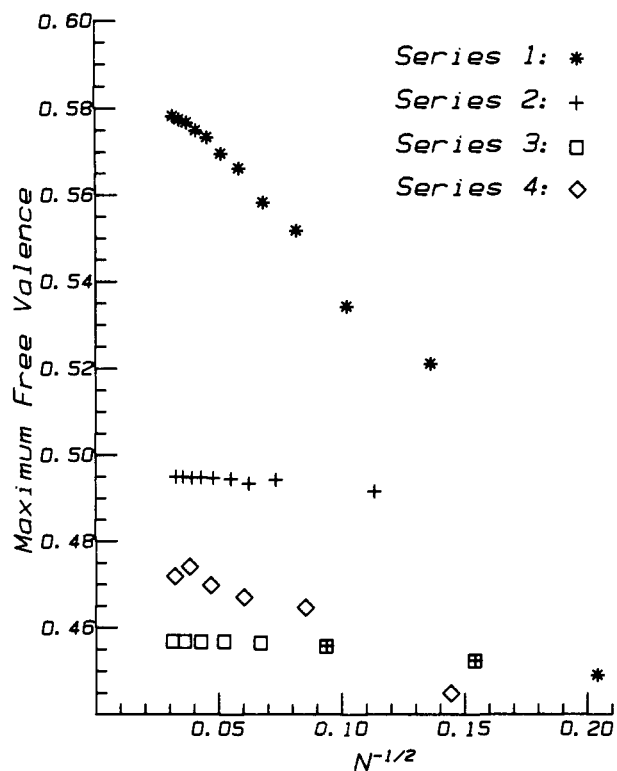


Figure 16. Maximum free valence for each molecule in the four homologous series as a function of molecular size.

to  $i$  minus the actual total bond order to  $i$ . This index has been used to correlate reactivity in free radical attack. It can predict relative ease of attack at different sites as well as variations in reactivity among different molecules.

In Figure 16 we show the maximum free valence  $F_{\max}$  for each of the molecules in our four series. In each case,  $F_{\max}$  occurs at the same positions as those predicted by PMO localization energies. These locations are shown in ref 10. Each series has a different limiting  $F_{\max}$  as  $N$  goes to infinity. In sharp contrast, PMO theory predicts a limiting localization energy of zero for all interior and edge sites. This seems physically unreasonable. Localization of a  $\pi$ -electron in the interior of a graphite layer is sure to result in a substantial loss of resonance energy. Consequently, while PMO theory is a useful indicator of relative reactivity at different positions in a single molecule, free valence should be a better parameter for correlating reactivity between different molecules. Figure 1 again shows the importance of edge structure. While the least stable series has an extremely high limiting  $F_{\max}$ , and thus high reactivity, the most stable has a limiting  $F_{\max}$  which is about the same as that for naphthalene. Very large, condensed polybenzenoid molecules with high-energy HOMOs need not be highly reactive toward free radicals and electrophiles.

#### 4. Summary

HMO theory provides a reliable semiquantitative description of the  $\pi$ -electron properties of very large graphite-like molecules possessing well-defined edges. By examining homologous series one can separate properties of atoms near the edge from those of atoms in the interior. In general terms, edge carbon atoms behave very much like those of normal polynuclear aromatic molecules, with properties depending strongly on the local structure. Phenanthrene-like edges are rather unreactive and thermodynamically stable. They are as susceptible to free radical and electrophilic attack as are structurally related positions in naphthalene and phenanthrene. Anthracene-like edges are

thermodynamically unstable and highly reactive, with properties comparable to those of the linear polyacenes.<sup>10</sup> Regardless of edge structure, interior carbon atoms situated only several bond lengths from an edge have properties (bond orders, free valence) not far from those of the interior carbon atoms in catacondensed polyaromatic molecules like coronene. A significant general finding for the molecules studied is that there is only a weak relation between the energy of the highest occupied molecular orbital and the reactivity of the most reactive position. For instance, while very large series 3 molecules (phenanthrene-like edges) will have higher HOMO energies than those of small series 1 molecules (anthracene-like edges), they will be far less reactive (cf. Figures 4 and 16). This HMO method predicts the thermodynamic stability is strongly influenced by edge type. In contrast, because they utilize local properties only, group additivity methods do not predict significant edge effects.

Wave functions, which describe overall molecular properties, separate into two distinct classes for molecules with reactive edges. Those of a more stable variety are qualitatively similar to those of an infinite plane and of the molecules with stable edges. Those of a less stable variety correspond to orbitals whose electron density are located primarily at the edges. The latter variety lead to a near zero band-gap, and the associated spectroscopic and electronic properties, for molecules of relatively small size. For example, a molecule with reactive edges containing 60 carbon atoms has the same band-gap as a molecule of the stable variety containing between 2000 and 2500 carbon atoms.

**Acknowledgment.** This research was supported by the Gas Research Institute and by the U.S. Air Force Office of Scientific Research.

#### Appendix. Calculation of Additive $\pi$ -Energies for Resonance Energy Reference Structures

In calculating additive  $\pi$ -energies by using the bond energy terms  $E_{ij}$ , Hess and Schaad<sup>11</sup> used an average of the individual additive  $\pi$ -energies of all possible Kekulé structures. This approach is clearly out of the question for our molecules; (e.g., the largest series 3 molecule we examined has  $10^{192}$  Kekulé structures). However, for the small molecules they examined, in no case were the additive energies of individual resonance structures of the same compound significantly different. Thus, a sufficiently accurate value for the additive energy could be calculated from only one of the many structures. However, it is possible to do better than this.

For a particular molecule of this type considered here, the total number of carbon-carbon double bonds is the same for all Kekulé structures and is easily determined. What must be established for one or more structures are the numbers of carbon-carbon double and single bonds along the edges of the molecule in which one or both carbons have an attached hydrogen atom. In our case these will be bonds of types  $\text{CH}=\text{CH}$ ,  $\text{CH}=\text{C}$ ,  $\text{CH}-\text{CH}$ , and  $\text{CH}-\text{C}$ . The total numbers of carbon-carbon edge bonds in our molecules are always even in number. We therefore arbitrarily assign these bonds to an alternating double and single configuration all around the molecule. The interior part of the remaining structure is always an even-alternant molecule with many resonance structures. All of its bonds are of types  $\text{C}=\text{C}$  and  $\text{C}-\text{C}$  (i.e., no attached hydrogens). By this approach it is easy to derive polynomial expressions for each series which give the numbers of the different types of bonds as a function of the generating index  $K$  shown in Figure 1. For example, we have with series 1 molecules,  $(\text{C}=\text{C}) = 3K^2$ ,  $(\text{CH}=\text{C}) = 6K$ ,  $(\text{CH}=\text{CH}) = 3$ ,  $(\text{C}-\text{C}) = 3K + 6K^2$ ,  $(\text{CH}-\text{C}) = 6K$ , and  $(\text{CH}-\text{CH}) = 3$ . The additive  $\pi$ -energies calculated in this manner are thus seen to be an average over all those particular Kekulé structures which have alternating double and single bonds around the perimeter of the molecule.